	CRDM
	Gripper Bellows
Failure Mode	Pin Hole
Failure Cause (Presumed)	Alkali Corrosion
Fractograph (SEM)	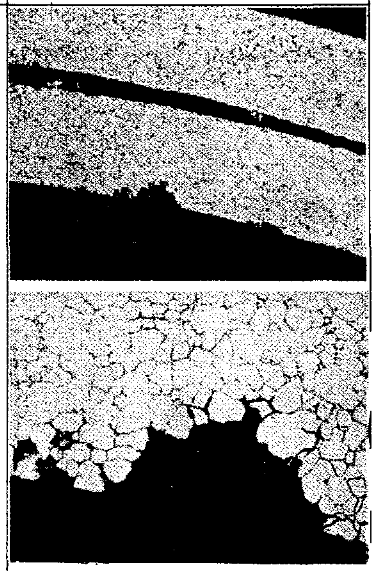

Photograph 3-1 Gripper Bellows Failure

DEVELOPMENT OF BELLOWS FOR IHX IN JAPAN

T. FUNADA, Y. TOMIOKA, S. NORIMATSU, T. OHTA, T. TAKAHASHI
Japan

Abstract

A bellows is installed at the outer side of the secondary sodium entrance nozzle of MONJU IHX as the absorber for the difference of thermal expansion between the pressure equipment and the piping.

A research and development program on IHX bellows was performed in the field of experiment and analysis for establishing the feasibility of IHX bellows under high temperature conditions.

This report consists of three sections, namely design profile, experimental tests and analysis of IHX bellows.

In the design profile a calculation of temperature distribution of bellows and stress analysis using a half convolution model are included. Basic tests such as non-destructive tests on the raw metal sheet and selection tests of welding conditions were performed. Some results of these basic tests, fatigue tests and sodium exposure tests are described in the research and development section of this report. Furthermore, analytical calculations led the correlations on the maximum stress between axial and some other loads.

1. Design Profile of Bellows for IHX of MONJU

1.1 Introduction

Design of IHX bellows of MONJU is now under development that means it is not fixed, however, brief outline of that design is to be explained here.

1.2 Configuration of IHX Bellows

Although final design of IHX Bellows will be modified, current design is shown in Figure 1-1. Further information is included in another paper "Fatigue Test Program of Bellows for IHX of MONJU". In Figure 1-1 you can see two types of bellows A and B. However, bellows B does not play a role as primary boundary, our current program mainly pays attention to bellow A which exists at entrance of secondary sodium. Drawing of bellows A is shown in Figure 1-2.

1.3 Design Condition

1)	Design Temperature	400°C (Normal) 250°C (Pre heating)
2)	Design Pressure	2.0 kg/cm^2 (Normal) -1.0 kg/cm^2 (Pre heating)
3)	Environment	Argon gas with sodium vapour (inner surface) Nitrogen gas (outer surface)
4)	Design Life	30 years
5)	Design Stroke	±40 mm
6)	Repeated Cycle of Stroke	∿ 2000
7)	Applicable Code	ASME Code Case N-47

1.4 Preliminary Strength Calculation

Preliminary strength calculation for 2 ply bellows by rule (JIS B8243) is prescribed here.

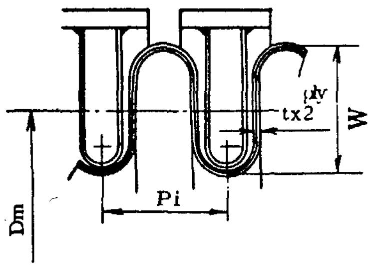

Design Pressure:	2 kg/cm^2
Height (W):	58.5 mm
Thickness (t):	1.5 mm
Pitch (Pi):	50.0 mm
Effective Dia. (Dm):	781.5 mm
Number of corrugation (n):	14
Stroke (Peak to Peak) Δx:	80 mm
Number of ply (C):	2

Calculation:

Stress in bellow can be obtained using following formula.

$$S_R = \frac{1.5E\ t\ \Delta x}{(Pi/2)^{0.5} \times W^{1.5} \times 2n} + \frac{PW}{100\ txc}$$

$$= \frac{1.5 \times 2 \times 10^4 \times 1.5 \times 80}{25^{0.5} \times W^{1.5} \times 2 \times 14} + \frac{2 \times 58.5}{100 \times 1.5 \times 2}$$

$$= 57.86\ kg/mm^2$$

Allowable cycle number Nf is as follows.

$$Nf = \left(\frac{563}{S_R}\right)^{3.5} = \left(\frac{563}{57.86}\right)^{3.5} = 2874$$

This satisfies the necessary cyclic life 2000.

1.5 Temperature Calculation of Bellows

To determine normal operating temperature of bellows, analysis using Finite Element Analysis Code MARC was carried on. Figure 1-3 shows steady state temperature distribution of bellows. Temperature of bellows is mainly governed by that of secondary inlet sodium, 325°C, and it could be found bellows temperature is nearly 310°C, that means far below from creep regime.

According to the data we concluded that design temperature of bellows is to be 400°C with some allowance.

1.6 Stress Analysis

Using general purpose finite element program MARC, stress analyses were performed under axial tension/compression load and internal pressure.

Figure 1-4 shows Stress Analysis Model. Analysis was performed for half of one convolution.

Figure 1-5 and Figure 1-6 shows results of the analyses for outer bellows.

Roughly speaking, maximum stress at the root of outer bellows are $23 \sim 24$ kg/mm^2 by axial compression 40 mm and $5 \sim 6$ kg/mm^2 by internal pressure 2 kg/mm^2. Design stroke is ±40 mm and design pressure is 2 kg/mm^2. That means total stress range is about $24 \times 2 + 6 = 54$ kg/mm^2 and shows good coincidence with the results calculated by Kellogg's formula.

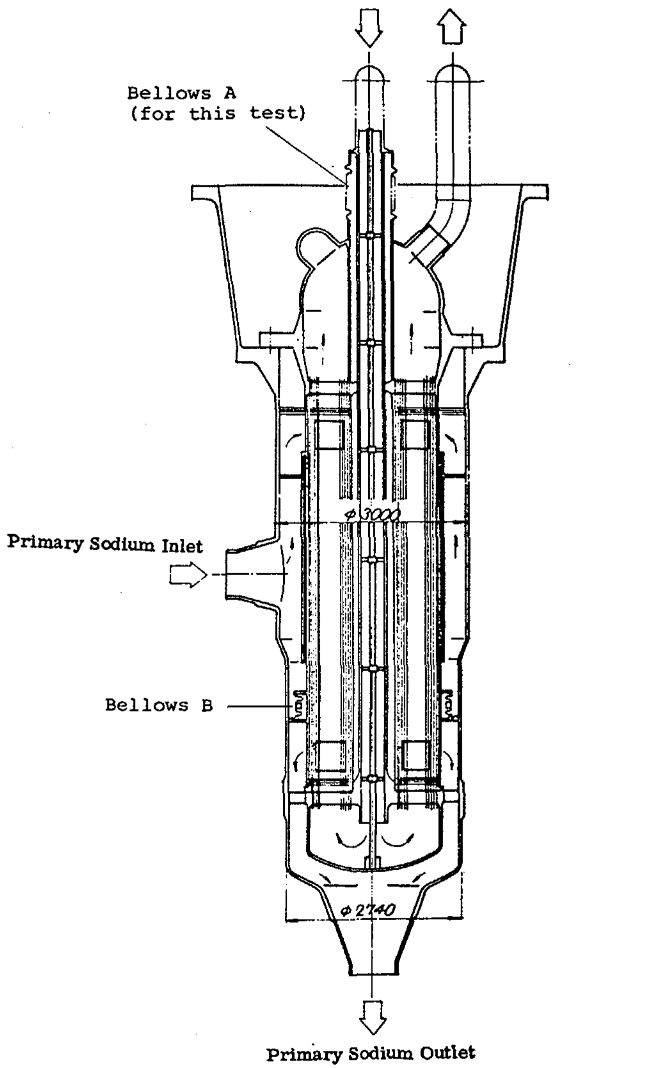

Figure 1-1 Intermediate Heat Exchanger of MONJU

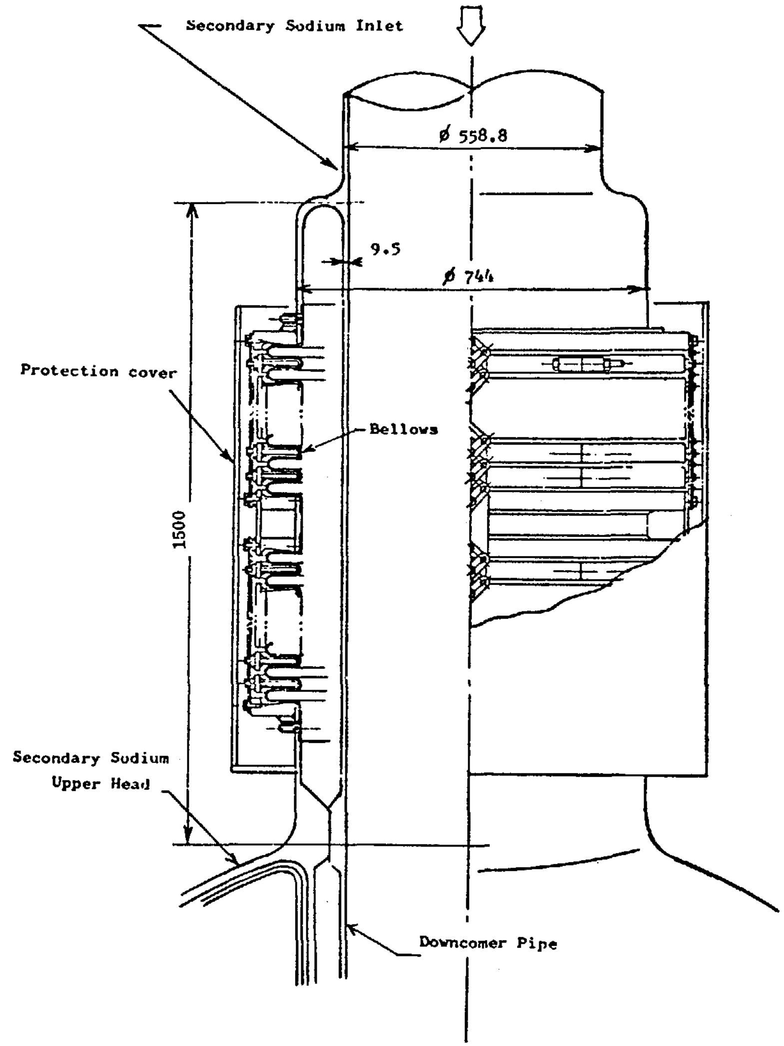

Figure 1-2 IHX Bellows A of MONJU

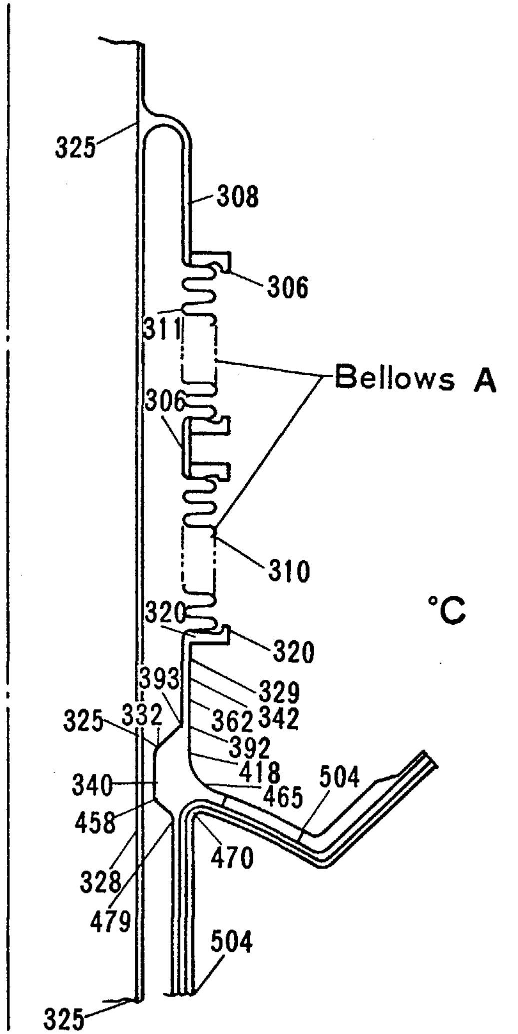

Figure 1-3 Temperature Distribution of Bellows Steady State.

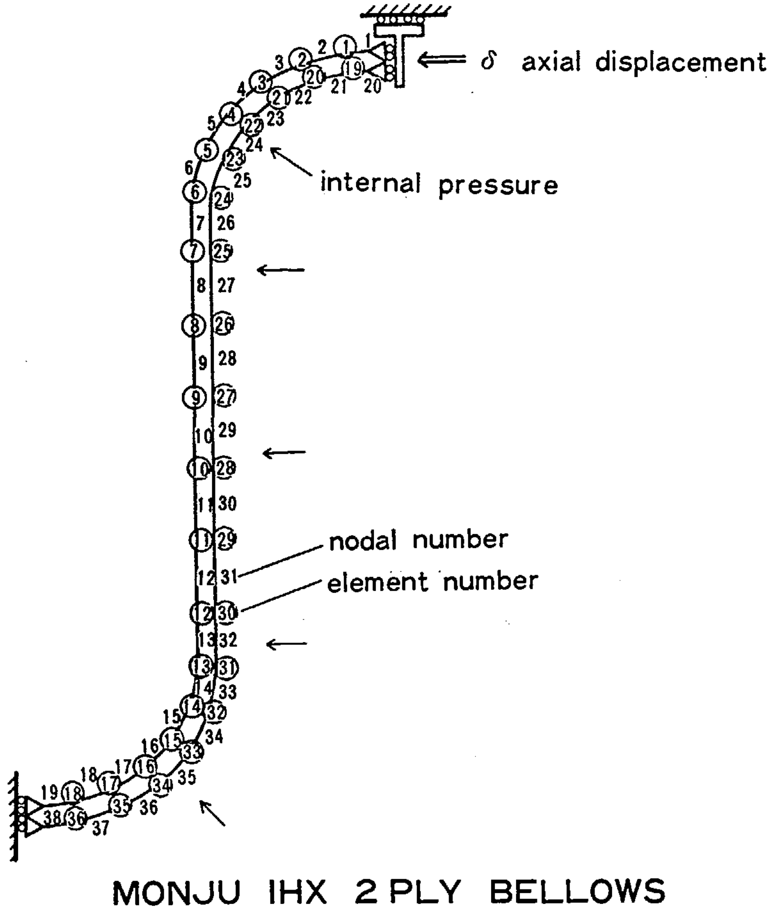

Figure 1-4 Stress Analysis Model

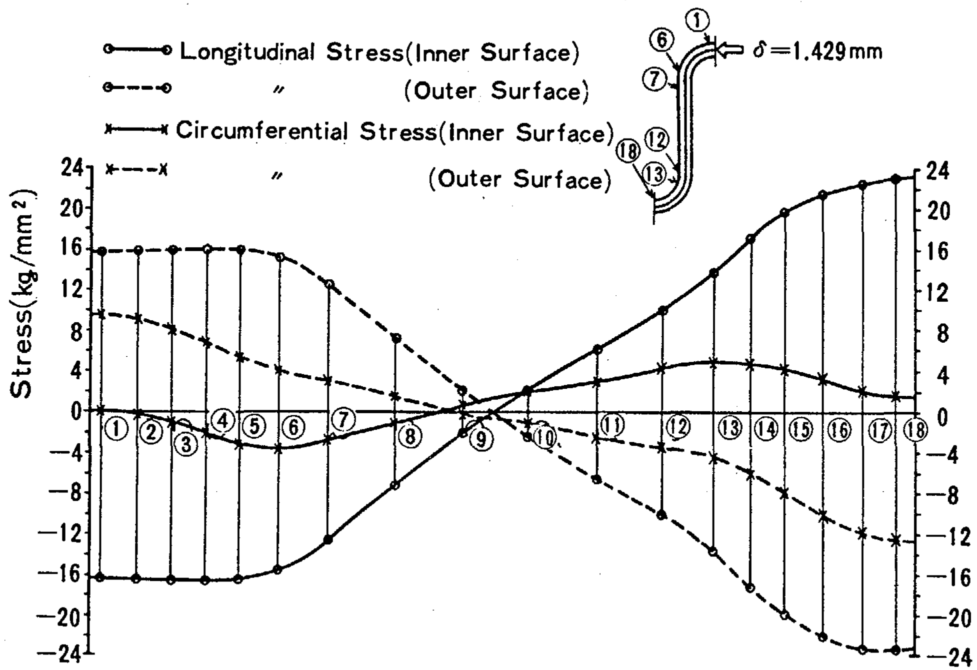

Figure I-5 Stress Distribution on Outer Bellows (Axial Compression)

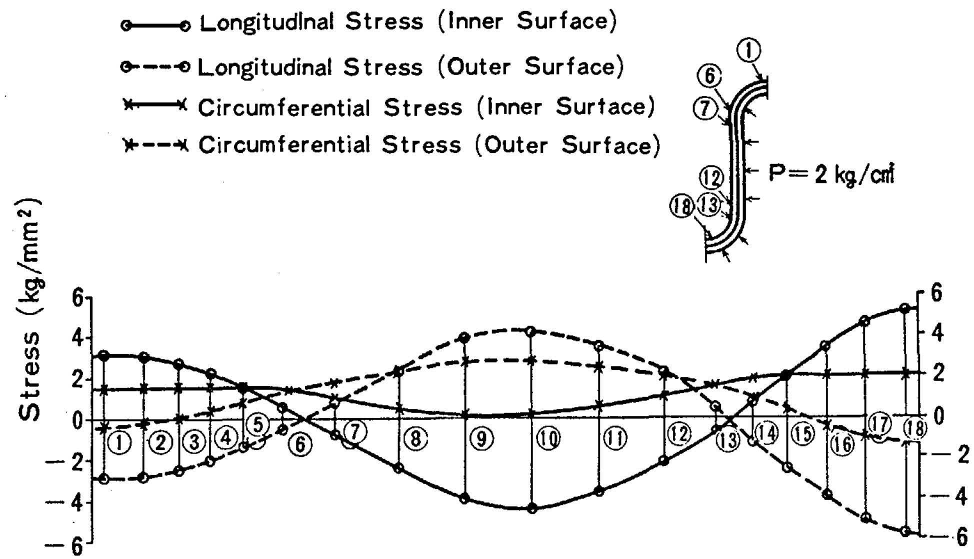

Figure I-6 Stress Distribution on Outer Bellows (Internal Pressure)

2. R & D Programs of Bellows for IHX of MONJU

2.1 Basic Test on Thermal Expansion Absorber

(1) Introduction

It is recommended to adopt the bellows for the absorber because the difference of thermal expansion between pressure vessel and piping becomes greater due to high operation temperature in the fast breeder reactor "MONJU". Especially, the bellows, which is used at the joint of the inlet piping and the upper end plate of the secondary sodium in the intermediate heat exchanger, requires a high quality and soundness because it forms the primary cover gas boundary.

The outline of the test results is as shown below.

(2) Sodium Adhesion Test

We conducted the sodium adhesion test (used water in place of sodium) on the specimens No. 1, 6, 7, 8 and 9 of different angle of bellows. As a result, it was discovered that less water was adhering to the specimen No. 8, and that the adhesion volume descreased when the water temperature rose. In other words, we discovered less water adhesion when an angle of the bellows is large.

(3) Non Destructive Test for the Bellows

In order to set up the standard of non-destructive test for bellows, we firstly conducted non-destructive test of raw pipe the bellows. The bellows was formed by the hydraulic press from raw pipe. As a result of non-destructive tests on this formed bellows, no defect was discovered.

Following test items were conducted.

1. Raw stainless steel sheet

   a. Ultrasonic test on stainless steel sheet.
   b. Liquid penetrant test on stainless steel sheet.
   c. Thickness measurement of stainless steel sheet. Thickness of sheet was measured by ultrasonic equipment.
   d. Mechanical test on stainless steel sheet.
   e. Microscopic test for non-metallic inclusion in steel.

2. After Bellows Forming

   a. Longitudinal weld seams in which 4 welding conditions for thin plate were selected and tested by ultrasonic test.
   b. Liquid penetrant test on longitudinal welded joint of formed bellows.
   c. Radiographic test on longitudinal welded joint of formed bellows.
   d. Helium leak test after assembly.
   e. Visual and dimensional test.
   f. Ferrite test.
   g. Eddy current test.

(4) Selection of Welding Condition

Regarding the experiment to select the thin plate welding conditions, we firstly selected 4 welding conditions for thin plate.

Non-destructive tests were conducted on welds of raw pipes which were welded under those conditions. It was judged that Tig welding (using filler metal of 0.6 mm dia) and Electric beam welding were satisfactory among the welding methods for the bellows raw pipe.

No.	Welding method	Filler wire
1	Automatic Tig.	1.2 mm dia. 316L
2	"	0.6 mm dia. "
3	"	non filler
4	Electric beam welding	"

We carried out following tests on longitudinal welded joints of cylinder prior to forming.

1. Prior to forming

   a. Radiographic test.
   b. Liquid penetrant test.
   c. Measurement of reinforcement of welded joints.
   d. Ferrite measurement on welded joints.

2. Destructive test of bellows

   a. Measurement of thickness for bellows convolution including parent metal and welded joints.
   b. Microscopic and macroscopic observation on the bellows specimen including parent metal and welded joints.
   c. Hardness measurement on the bellows convolution.
   d. Mechanical test for root, disc and crest of bellows convolution including parent metal and welded joints.
   e. After forming and heat treatment, welded joints of bellows was tested by ferritescope.
   f. Corrosion test of bellows.

(5) Mechanical Strain Measurement

We measured the bellows stress distribution by measuring the strain. On the other hand, we made the stress analysis by finite element method, compared it to the measurement, and learned that a tendency in both case agreed. There was some error between the measured value and calculated value because an effect of the reinforcing ring and a factor of 2 ply were unable to be reflected in the calculation.

We measured the bellows stress distribution by measuring the stress-strain. Test condition for expansion joint adopted for strain measurement are as shown below.

1st		2nd		3rd	
internal pressure	movement mm	internal pressure	movement mm	internal pressure	movement mm
0	0	2	0	0	0
0	+10	2	+10	0	+10
0	+20	2	+20	0	+20
0	+10	2	+10	0	+10
0	0	2	0	0	0
0	-10	2	-10	0	-10
0	-20	2	-20	0	-20
0	-10	2	-10	0	-10
0	0	2	0	0	0

Convolution height: 60 mm
Convolution pitch: 50 mm
Inside diameter: 720 mm
Nominal thickness: 1.5 mm
No. of convolution: 5 mm

No. of Piles: 2
Material: JIS SUS 316

Bellows was fit with reinforcing ring.

Strain gauges were attached to the inside surfaces of bellows convolution including crest, disc and root as shown in Figure 2-1. Test results are shown in Figure 2-2.

In order to proof against leakage from inlet in which lead wire of strain gauge was inserted, inlet was sealed tightly by special devices.

Measurement equipment
Strain gauge: 3 direction (120 ∿ 350 ohm)
Adhesion: Visca
Measurement equipment: Static strain tester

2.2 Fatigue Test Program of Bellows for IHX of MONJU

(1) Introduction

Because of severe environmental effects under elevated temperature condition and required reliability for IHX bellows we think it is necessary to perform full size mock-up static and fatigue tests of the bellows.

In this report are described the facilities, procedures and results of those tests.

(2) Testing Facility

(a) Fatigue Test Machine

Fatigue test machine is designed to give several kinds of loading and deformation to tested bellows, i.e. tension - compression, torsion, bending at room temperature and elevated temperature in liquid sodium environment.

Specifications of fatigue test machine are as follows:

1) Tension - Compression

Control item: load or displacement

Control wave form: sine wave, triangular wave, rectangular wave, lump wave, programmed wave

Cycle: 0.001 Hz - 0.04 Hz
Stroke: ±100 mm
Loading capacity: ±30 ton (±45 ton for static)

2) Torsion

Control item: displacement (constant holding)
Torsional moment: 0 - 9 ton-m

3) Bending

Bending angle: 1°, 1.5°, 2°

4) Excentricity: 0 - 20 mm

(b) Bellows for Testing

Totally 9 full size bellows with bolted flanges at both ends for settlement onto fatigue machine are prepared.

Bellows are made of stainless steel 316, and have 2 piles of which each thickness is 1.5 mm. Number of corrugation is 14 (7 x 2).

Design condition of this bellows is also explained in Section 1. "Design Profile of Bellows for IHX of MONJU".

(3) Procedure of Test

(a) Strain Measurement

To obtain basic data, strain guages are attached onto inner and/or outer surfaces of 3 bellows. Among them 2 bellows are attached with strain gauges for elevated temperature. Strains at several locations of bellows were measured under various condition of both end displacements.

(b) Fatigue Test

Purpose of fatigue test can be devided into two phases. One is to show reliability under design fatigue cycle i.e. 2,000 cycles. And another one is to obtain actual life of bellows under design fatigue condition.

6 bellows are available for fatigue tests under design temperature and loading conditions.

Prior to fatigue test, the bellows set in the pot is to be heated by electric heater settled in thermal insulation and then liquid sodium is filled up testing loop from mother loop including tested bellows.

(4) Test Results

(a) Strain Measurement

Results of the test are shown in Figure 2-3 ∿ 2-6.

Figure 2-3 shows longitudinal stress distribution of tested bellows without reinforcing ring at room temperature. It can be seen that maximum stress is around 25 kg/cm^2.

Figure 2-4 shows the same kind of stress distribution at 400°C. Averagely, the measured stress is about 15% lower than those at room temperature.

Figure 2-5 shows the stress distribution of bellows with reinforcing ring at room temperature. Results show significant difference between the stress value at the crests and roots. This may be caused by the constraint of deformation at the root of bellows by reinforcing ring.

Figure 2-6 shows stress change during increase and decrease of axial deformation of bellows and is a good explanation of the results above.

The results of the strain measurement test are summarized as follows.

1) Maximum stress appeared at the convolution crest of inner bellows and the convolution root of outer bellows. When bellows was extended and compressed the displacement by 40 mm (design condition), maximum stress observed at the convolution crest of inner bellows and the convolution root of outer bellows reached 27 ∿ 29 kg f/mm^2.

2) Stress observed at 400°C was 15% below those at room temperature.

3) Bellows with and without reinforcing rings indicated normal extension and compression at room temperature and 400°C.

4) No significant difference was observed between stress in dynamic test and those in static test in the frequency region from 0.004 to 0.04 Hz.

(b) Fatigue Test I

Test I shown on Table 2-1 has been already completed. After the respective fatigue tests under 400°C and axial deformation by ±40 mm with or without static torsion, bending and excentricity, following examinations were performed.

(i) Helium leak test
(ii) Dye penetrant examination
(iii) Material test
(iv) Thickness measurement etc.

However, no problems could be found for all cases and all bellows tested showed no imperfectness.

(c) Fatigue Test II

According to the results of strain measurement and Fatigue Test I, we got following conclusions for reinforcing ring.

(i) Stress at the crest of the bellow is concentrated by reinforcing ring under axial compression. (not for bellows without reinforcing ring.)

(ii) No differences of fatigue strength could be found under design fatigue conditions.

Furthermore, from the stand point of Inservice Inspection it is desirable to delete the reinforcing ring for MONJU bellows.

According to this judgement we determine that Fatigue Test II is to be done by using bellows without reinforcing ring.

2.3 Sodium Exposure Tests of the Thermal Expansion Absorbers (bellows) for the Intermediate Heat Exchangers for "MONJU"

In the intermediate heat exchangers (IHX) for "MONJU", entrance nozzles from the secondary coolant systems are connected by bellows with the upper shells of IHX to absorb the tortion and thermal expansion, due to the installation and operation of the system. The bellows which were fabricated for the thermal expansion absorbers were exposed to sodium at 550°C for 5000 hr, and examined the effects of sodium on the mechanical properties of the bellows. Cyclic strains corresponding to the design values were applied to the specimens taken out of the bellows at the speed of 1 cycle/hr in sodium. The results obtained are as follows:

(1) No marked differences in microstructures, chemical compositions, hardness and tensile properties at high temperature were observed between as received, sodium exposed and cover gas (argon) exposed bellows.

(2) Heat treatments after the fabrication contributed to the homogeneity of the microstructure and the relaxation of residual stress of the bellows.

(3) The tensile properties of the weld metals do not differ from those of base metals after sodium exposure.

(4) The difference in cold work, i.e. the shapes of the bellows do not affect the microstructures and tensile strengths after sodium and cover gas exposure.

Table 2-1 Planned Bellows Test

	Load combination	Repeated cycle	Number of tested bellows	reinforcing ring
I	Tension-Compression	2,000	2	Yes & No
	T-C with Torsion	2,000	1	No
	T-C with Bending	2,000	1	No
	T-C with Eccentricity	2,000	1	Yes
II	T-C	to failure about 40,000 cycles (calculated by Kellogg's formula)	1	No

(C) Schedule

Fatigue Test Facility	June, 1978
Static Test	Oct., 1978
Fatigue Test I	Aug., 1979
II	Early 1980

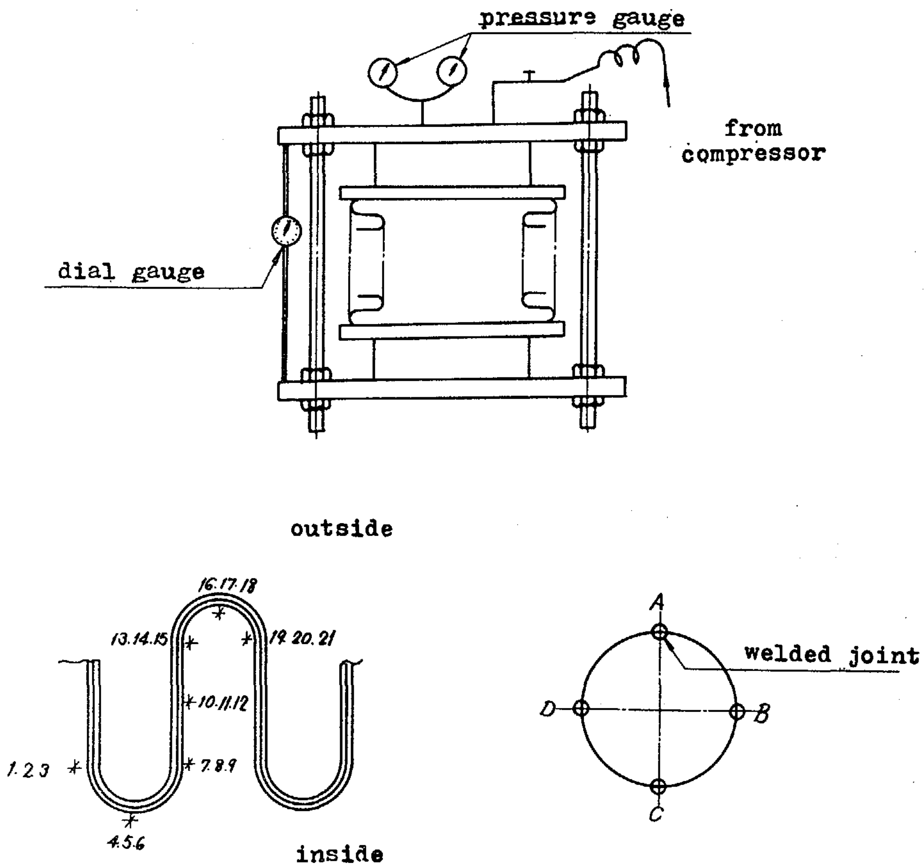

Figure 2-1 Mechanical Strain Measurement

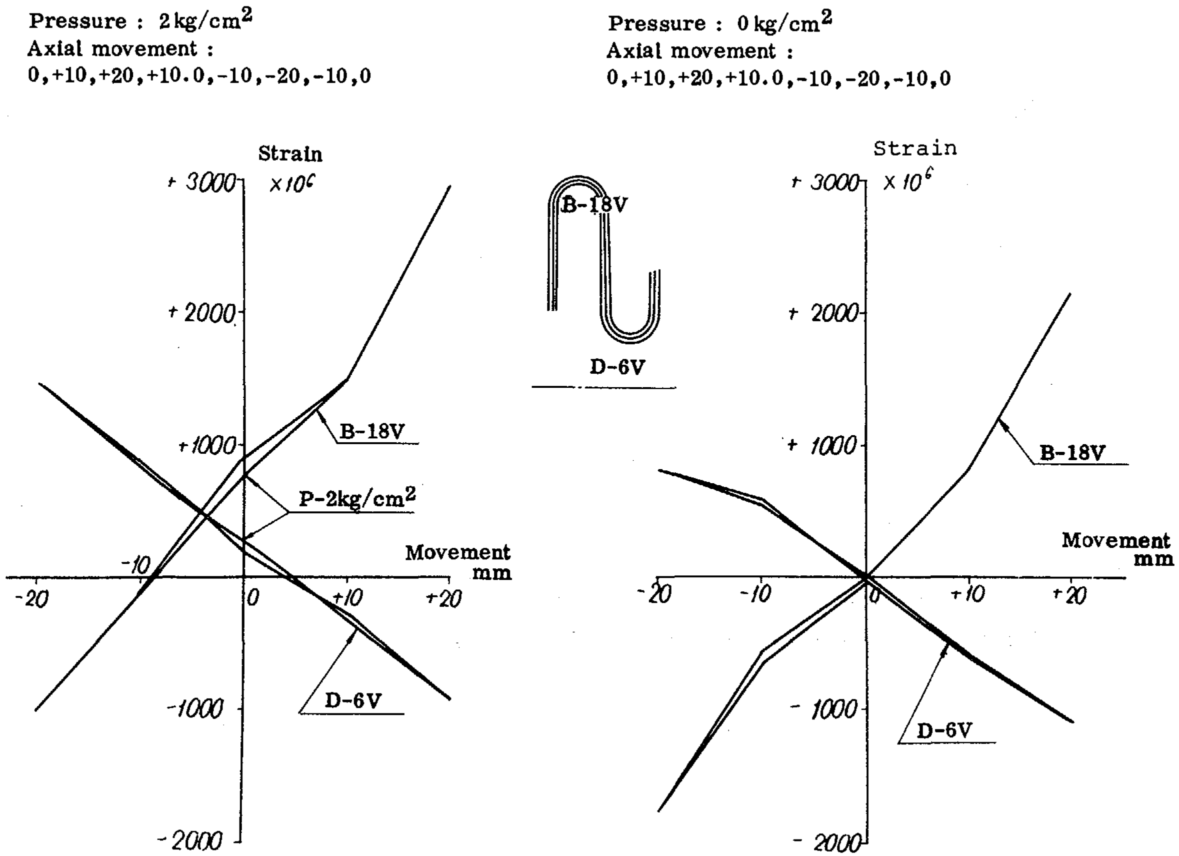

Figure 2-2 Results of Strain Measurement

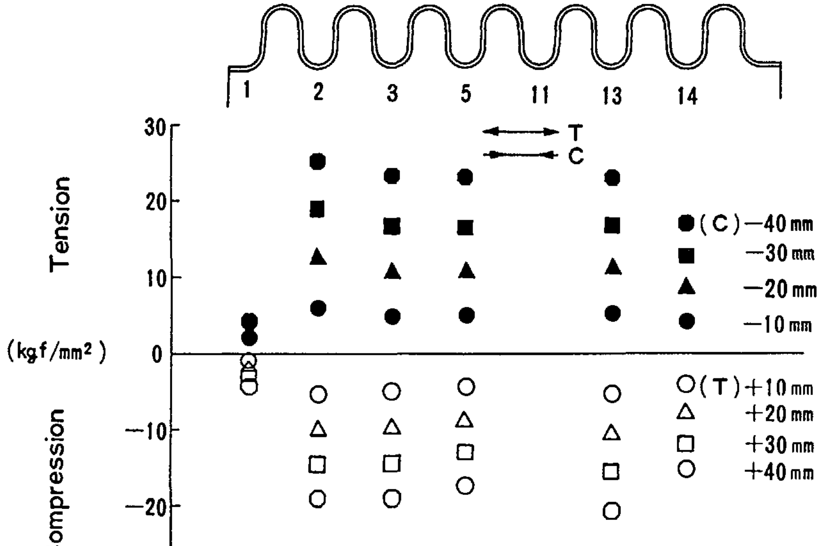

Figure 2-3 Longitudinal Stress Distribution
(without reinforcing ring, at room temperature)
(High temperature strain gauge)

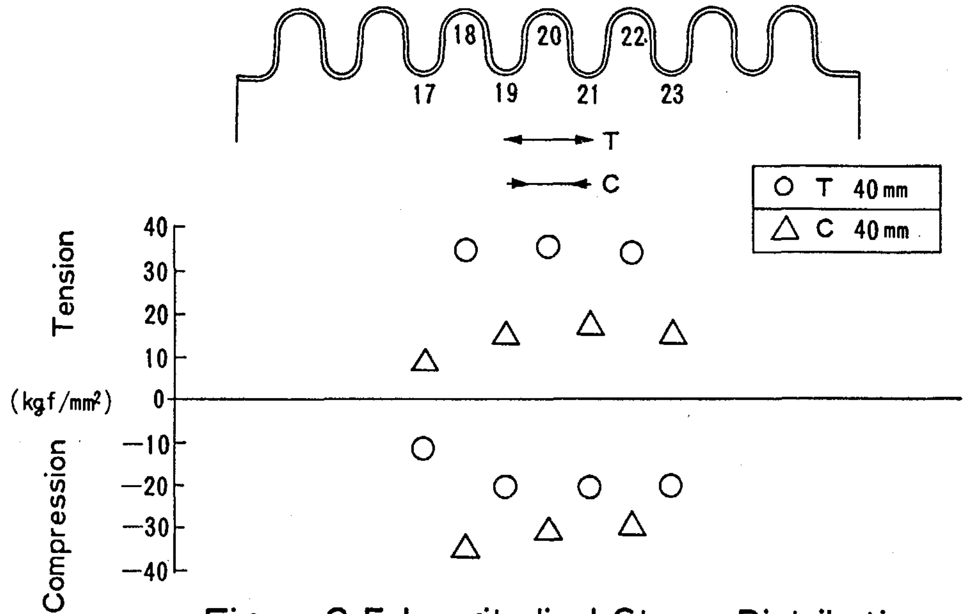

Figure 2-5 Longitudinal Stress Distribution
(with reinforcing ring, at room temperature)

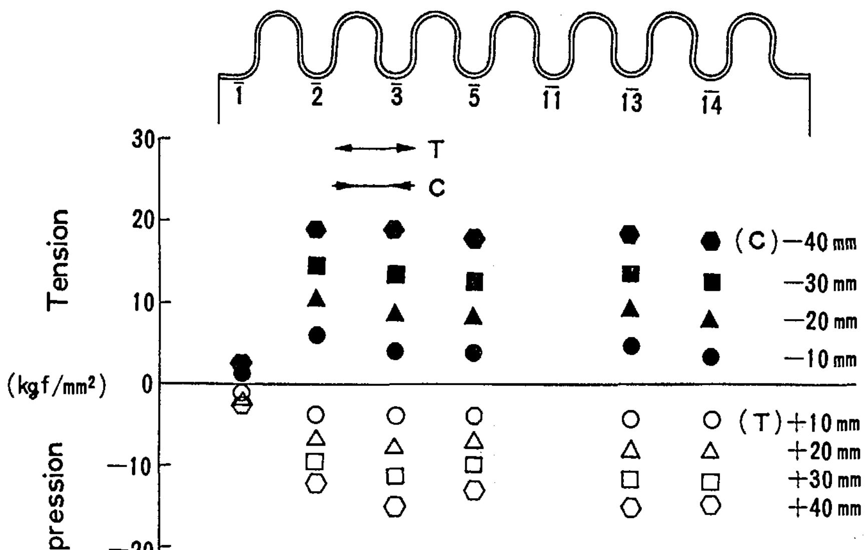

Figure 2-4 Longitudinal Stress Distribution
(without reinforcing ring, at 400°C)
(High temperature strain gauge)

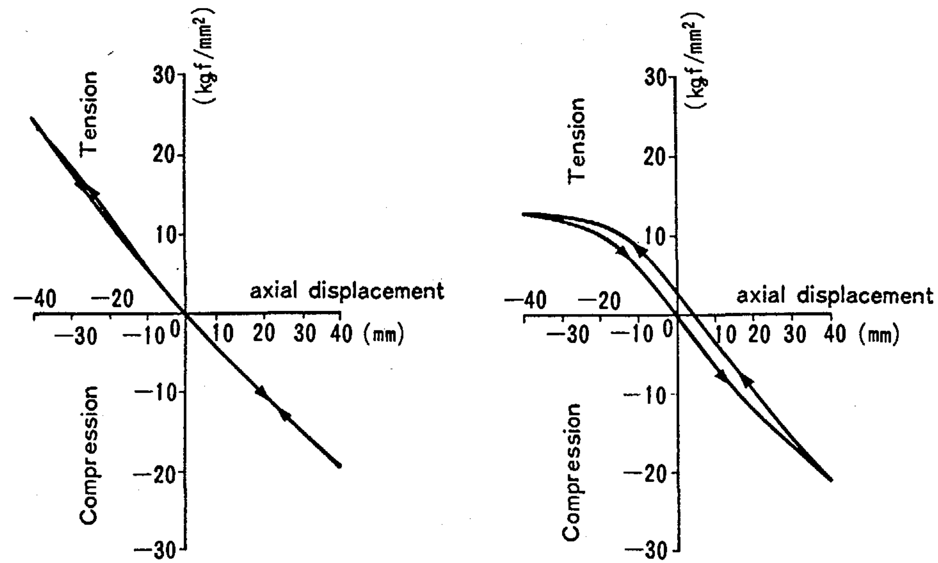

(1) without reinforcing ring

(2) with reinforcing ring

Figure 2-6 Longitudinal Stress at the root of Inner ply

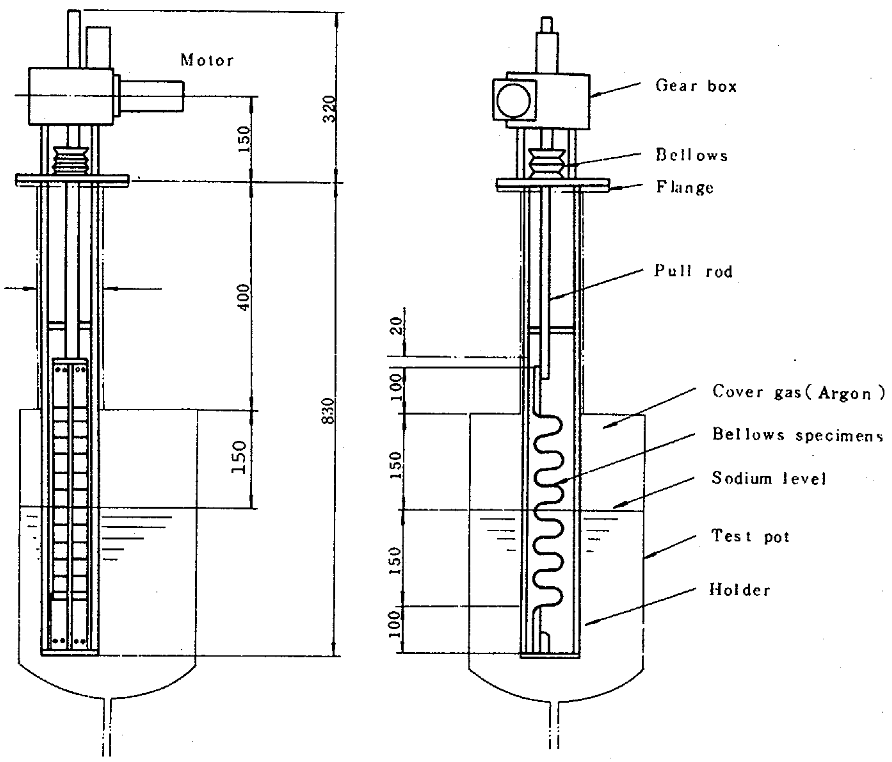

Figure 2-7 General Assembly of Specimen Holder.

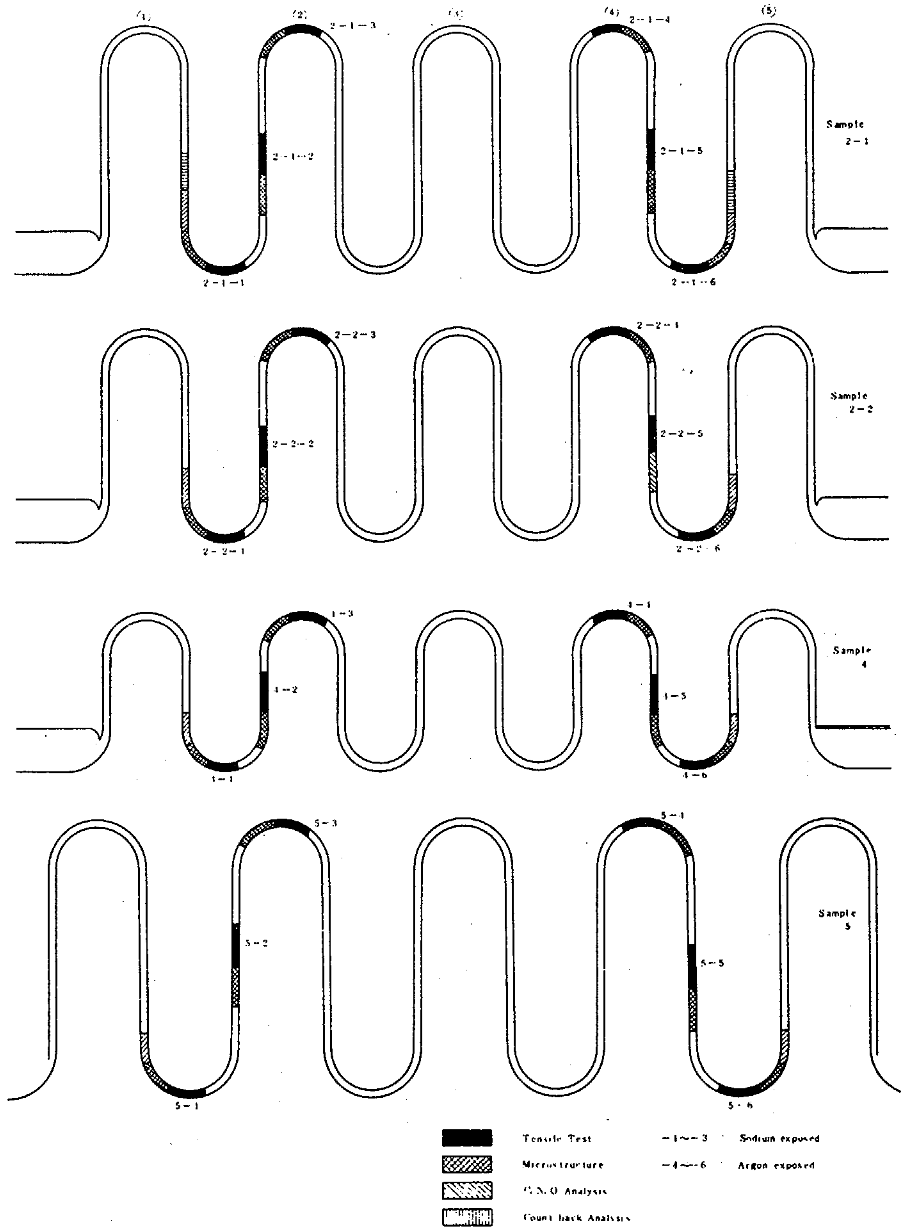

Figure 2-8 Post Exposure Test Sections of Samples.

3. Analysis of IHX Bellows

3.1 Introduction

It is anticipated that not only axial loads but also non-axisymmetrical loads including bending, torsion and shear are exerted on IHX (Intermediate Heat Exchanger) bellows. Behaviour of the bellows occurred by such loads and stress distribution need to be clarified. If the maximum values of stress under such loads are obtained corresponding with the axial loads needed to generate the said stress values is clarified, the equivalent axial loads corresponding to non-axisymmetrical loads can be defined, which will be effectively used for setting the conditions for design and experiments.

3.2 Analytical Model and Conditions

The specifications of the subject IHX bellows are as shown in Table 3-1, and it is equipped with accessories including reinforcing ring and neck ring. In the analysis, these accessories are excluded and double-boundary model is treated as single-boundary model. Furthermore, the analysis is based on 7 convolutions and uniform temperature of 400°C. And the internal and external pressure and the temperature distribution in the direction of plate thickness are disregarded. The aforementioned 3 kinds of loads were handled respectively given by enforced displacement. (See Figure 3-1)

Finite Element Method Program "ANSYS" was used for the analysis and the element STIFF61* capable of performing analysis by applying non-axisymmetric load on axisymmetric structure model was used.

In Figure 3-2 are shown the analytical model and divided mesh arrangement are shown. The maximum number of elements is 250.

* Axisymmetric Conical Shell Element with Non-Axisymmetric Loading

3.3 Results of Analyses

Examples of the displacement on the center of bellows where axial load (MODE 1), bending load (MODE 3) and shearing load (MODE 4) are applied are shown in Figure 3-3 through Figure 3-5. In the case of bending load, the distribution of axial displacement is unsymmetric between upper part and lower part. This is because the length of end-tangent is not identical at the upper end and lower end.

Since there was observed no axial displacement in the case of torsional load (MODE 2), description has been omitted.

The explanation of stress and the symbols used in this analysis are shown in Figure 3-6. The symbols used in the stress distribution diagram have the following meanings.

- S1: Meridional stress (External surface)
- S2: Meridional stress (Internal surface)
- TH1: Circumferential stress (External surface)
- TH2: Circumferential stress (Internal surface)
- SI: Stress intensity

Distribution of meridional stress and circumferential stress to axial load, bending load and shearing load is shown in Figure 3-7 through Figure 3-12.

And distribution of stress intensity to the said 4 kinds of loads is shown in Figure 3-13 through Figure 3-16.

The maximum value of stress intensity in the case of axial load, torsional load and bending load shows no wide scattering in each convolution, but in the case of shearing load, the value is the maximum at both ends and the minimum at the center, and large scattering is shown between each convolution. In the case of bending load, the distribution of stress intensity is not symmetric in longitudinal direction. This is because the lengths of end-tangent part at both ends are not identical. The relation between the maximum stress intensity and each load is shown in Figure 3-17.

By using this diagram, the corresponding relation between non-axisymmetric loads including torsional load, bending load and shear-load and axial loads can be induced from the standpoint of the maximum stress intensity. For example, a solution can be given to a question, "What is the axial load y (mm) required, if the maximum stress is equal to one generated by bending load x (degree) ?" Using proportional constant k in the equation y = k.x, following correlations are obtained for each load.

$$L_a = k_B \cdot L_B$$
$$L_a = k_T \cdot L_T$$
$$L_a = k_L \cdot L_L$$

Where L_a: axial load (mm), L_B: bending load (degree),
L_L: shearing load (mm), L_T: torsional load (degree)

The proportional constants k_B, k_L and k can be obtained as follows:

k_B = 16.17 (mm/degree)
k_L = 10.78 (mm/mm)
k_T = 184.7 (mm/degree)

And when each of load L_a and L_B is given, the maximum stress intensity SI_{max} generated in bellows can be given by the following formula.

SI_{max}	= 0.97 x L_a	(kg/mm^2)
	= 15.68 x L_B	(")
	= 10.46 x L_L	(")
	= 179.26 x L_T	(")

3.4 Conclusion

The results obtained by the analysis are summarized as follows.

(1) Since torsional load and shearing load are apt to generate a comparatively large stress, structural consideration is needed for the design of using bellows. Furthermore, these kinds of loads should be minimized in layout of piping.

(2) In the case of shearing load, a large stress is generated at the ends of bellows and a small load at the center, and scattering of stress value between each convolution is large. It is important that the analytical result shows bellows failure is likely to occur at the end parts.

(3) The axial load for generating the stress intensity equivalent to the maximum stress intensity generated by torsional load, shearing load and bending load respectively could be obtained. It is useful for substituting the experiments of non-axisymmetric loads by axial loads.

(4) The non-axisymmetric loads and the maximum stress intensity in this IHX bellows can be obtained by the following formulas.

SI_{max} (kg/mm^2)	= 0.97 x L_a	L_a: Axial load (mm)
	= 15.68 x L_B	L_B: Bending load (degree)
	= 10.46 x L_L	L_L: Shearing load (mm)
	= 179.26 x L_T	L_T: Torsional load (degree)

Table 3-1 Specifications of IHX Bellows

1. Material   SUS 316

2. Design Conditions
   a) Pressure   −1~2 kg/cm^2g
   b) Temperature   400 °C
   c) Axial Stroke   ±40 mm
   d) Allowable number of loading   2000 cycles

3. Configurations
   a) 2 ply (1.5t×2)
   b) Inner diameter   720 mm
   c) Height of convolution   61.5 mm
   d) Number of convolution   7

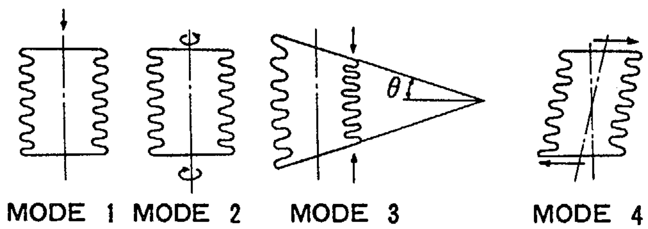

MODE 1	Axial load	20 mm
MODE 2	Torsional load	3 degrees
MODE 3	Bending load	5 degrees
MODE 4	Shearing load	10 mm

Figure 3-1 Loading for Analysis

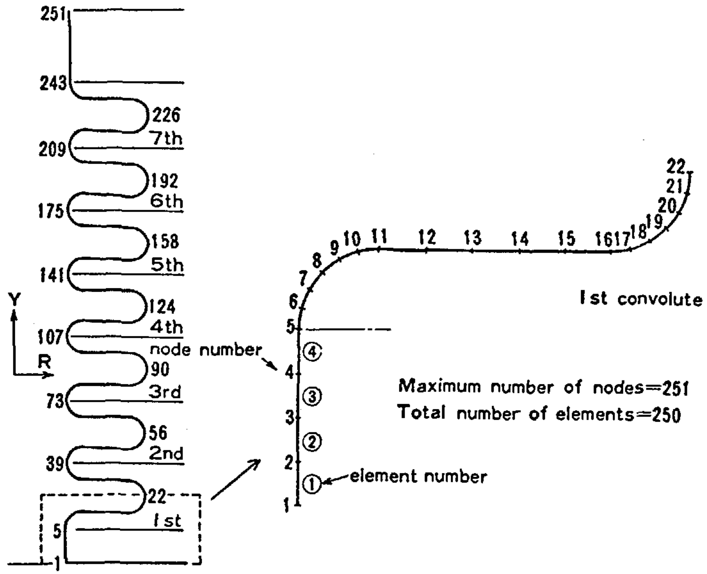

Figure 3-2 Mesh Arrangement used in analysis.

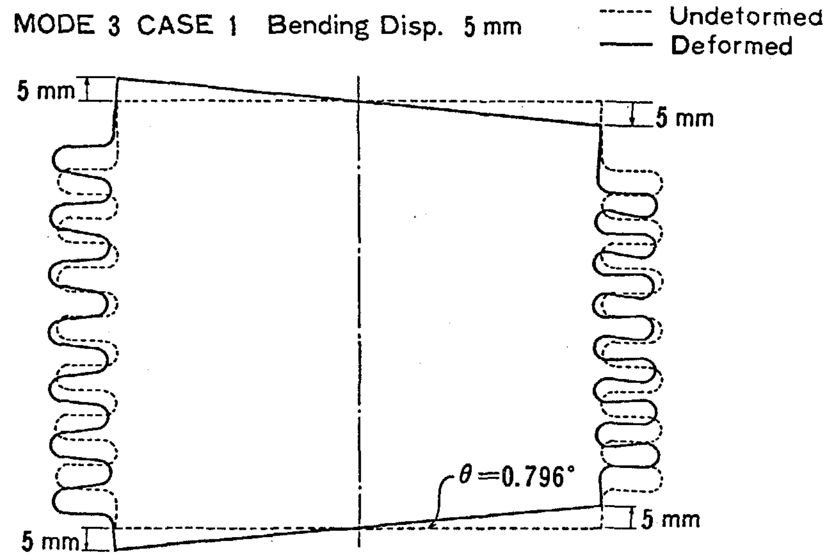

Figure 3-4 Deformation of bellows for bending loading

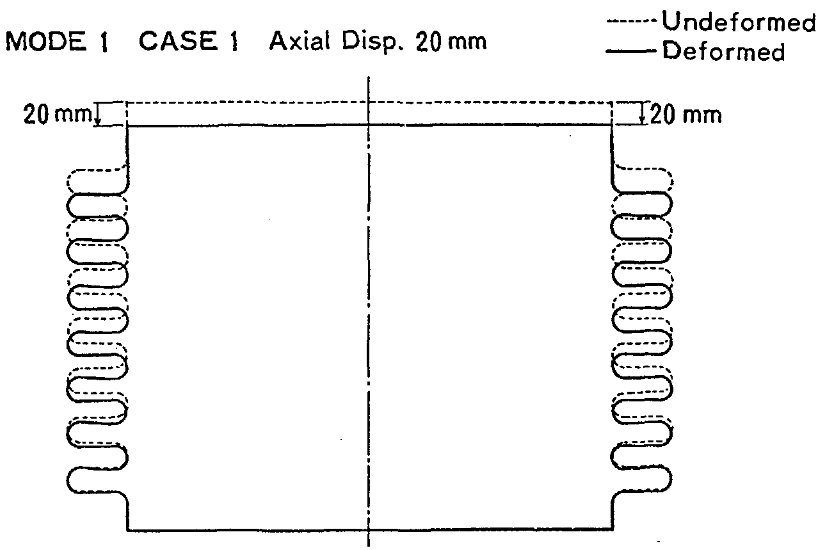

Figure 3-3 Deformation of bellows for axial loading (20 mm)

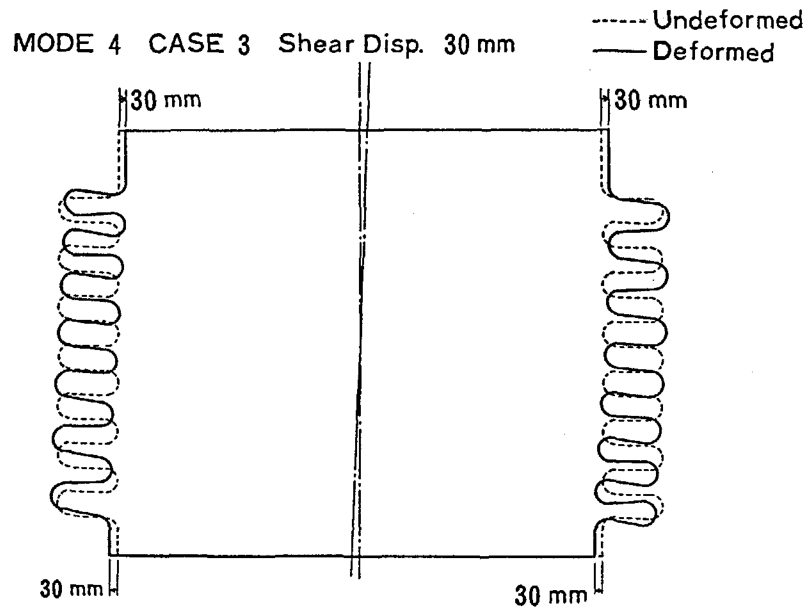

Figure 3-5 Deformation of bellows for lateral loading. 30 mm

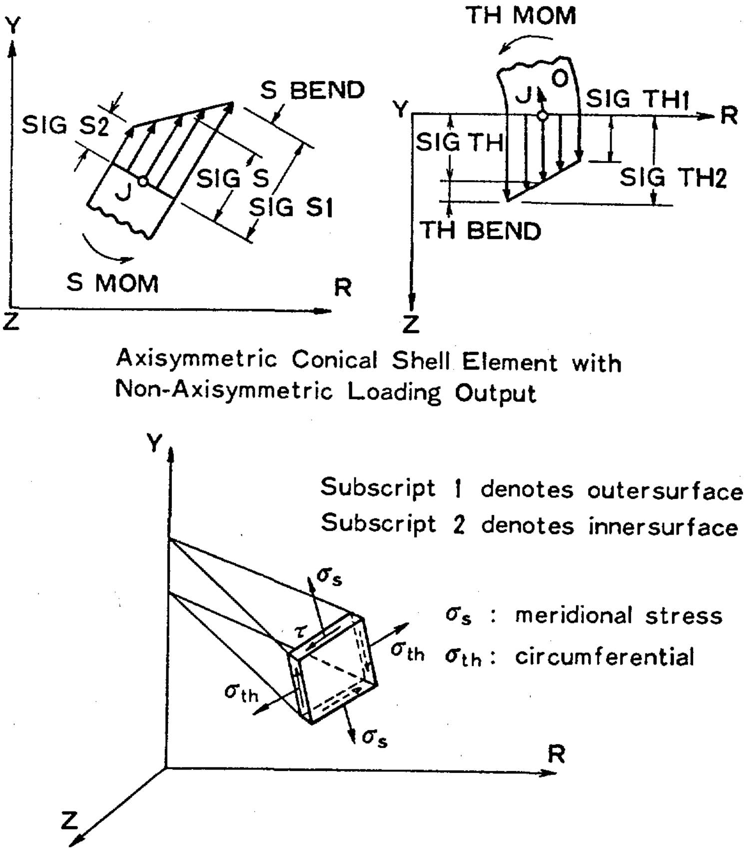

Figure 3-6 Explanation of Stress.

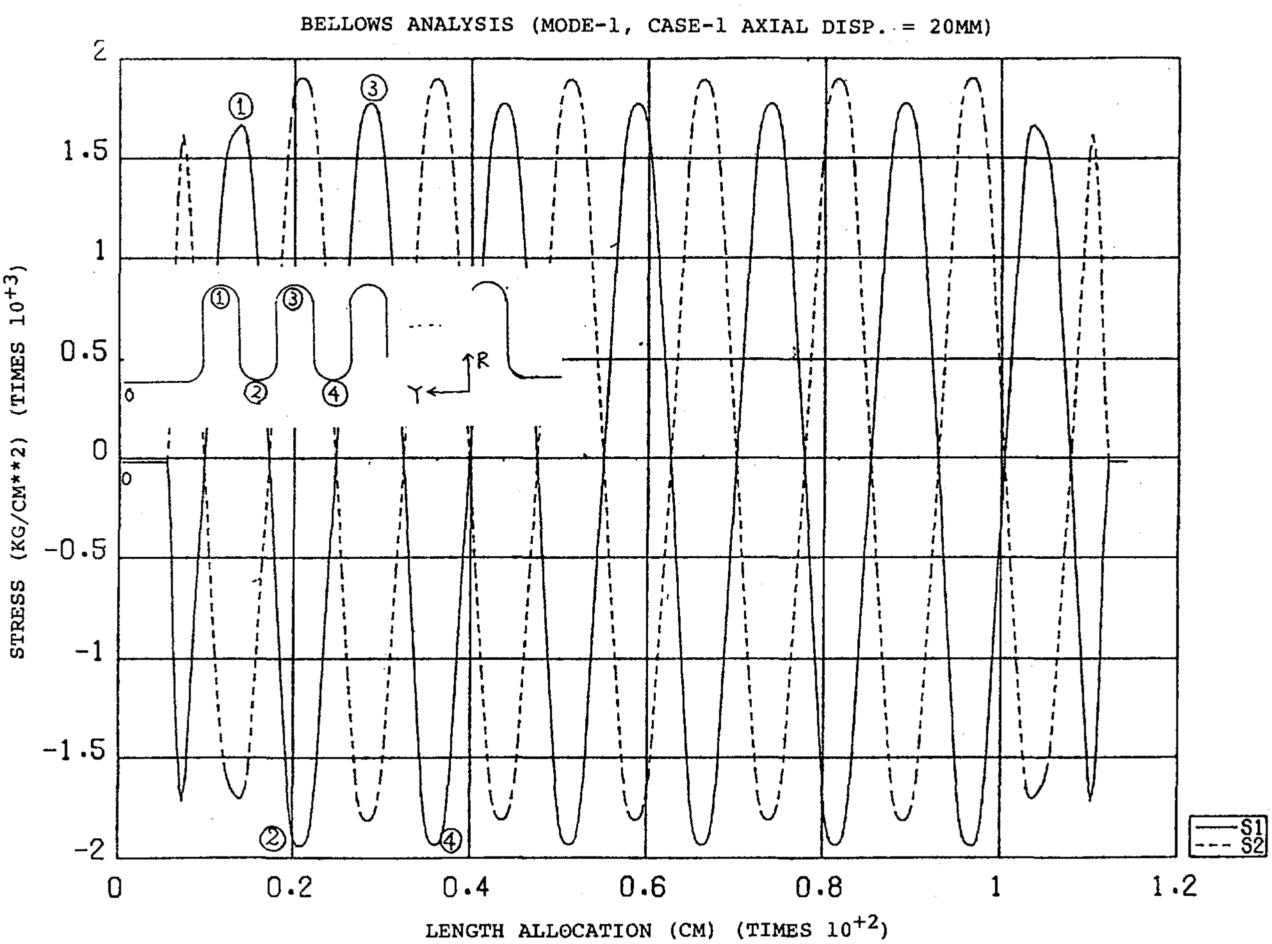

Figure 3-7 Stress distribution for axial loading.

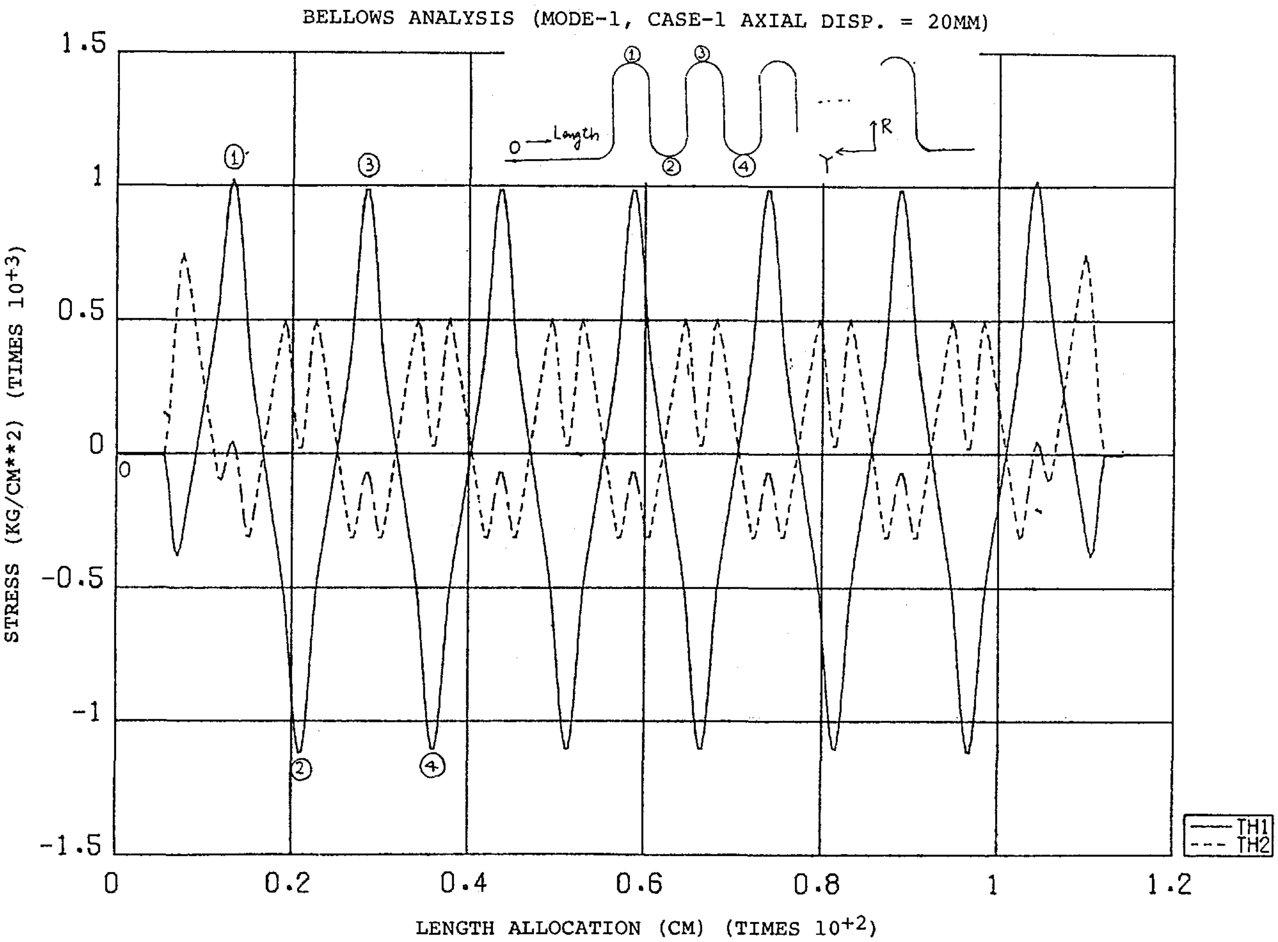

Figure 3-8 Stress distribution for axial loading.

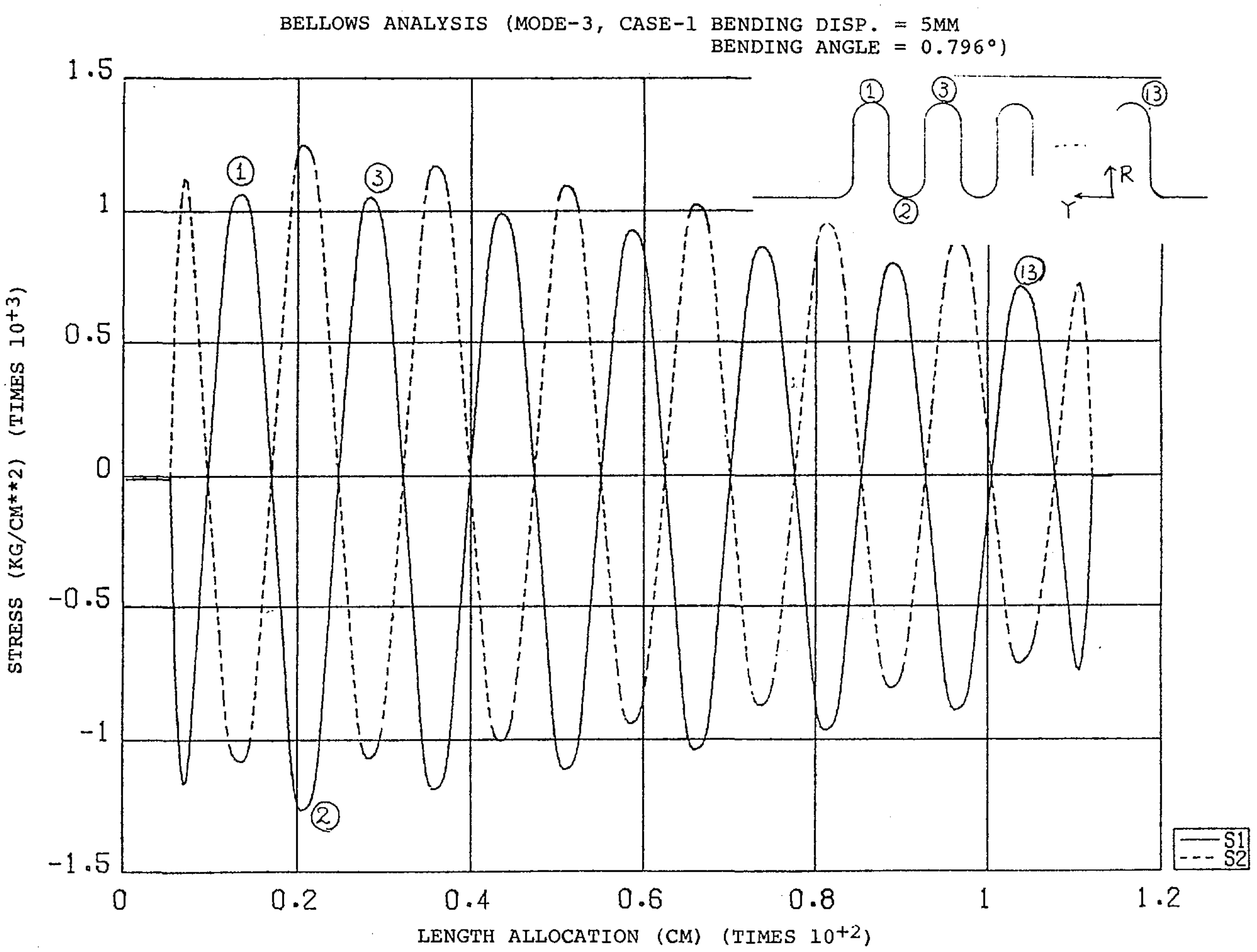

Figure 3-9 Stress distribution for bending loading.

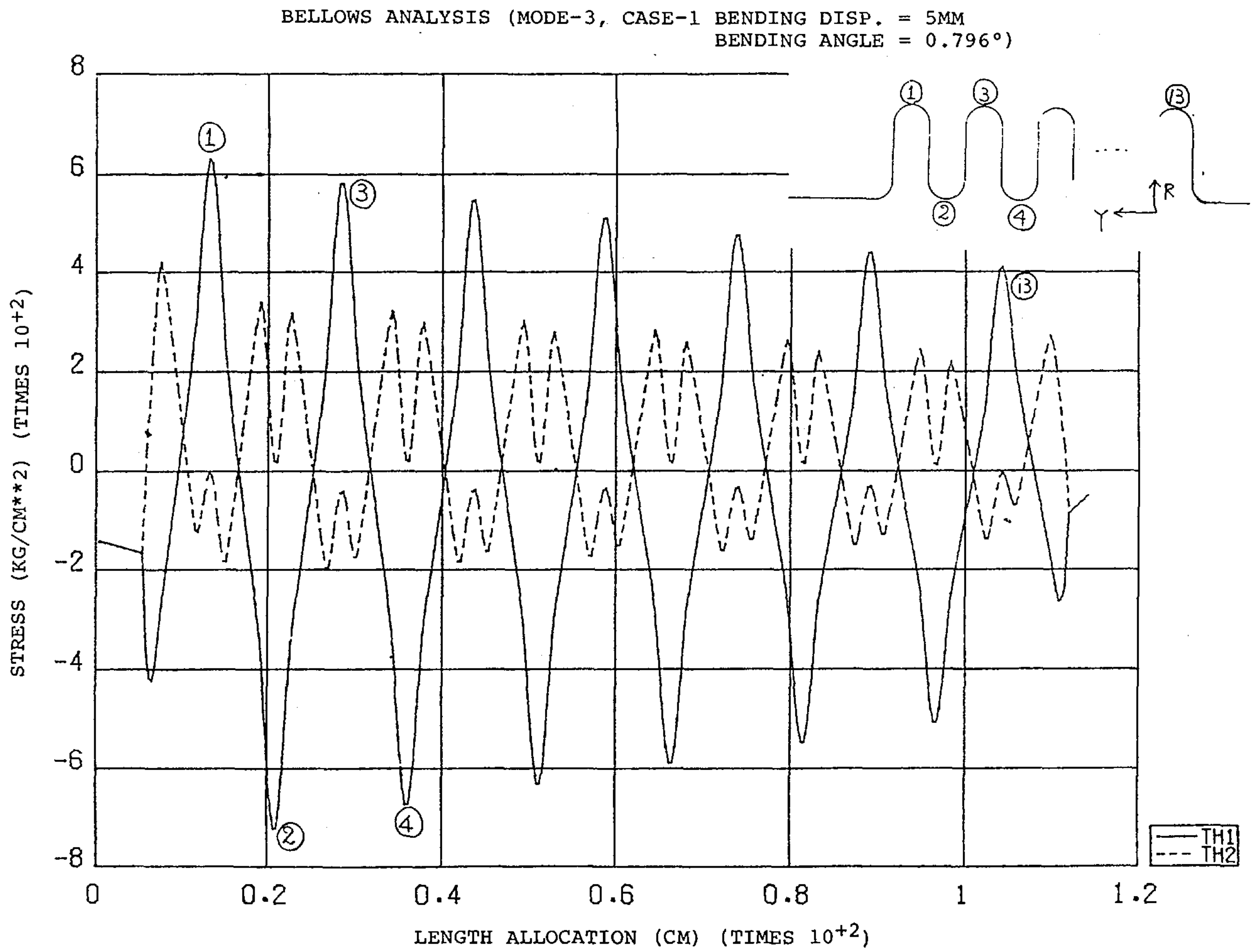

Figure 3-10 Stress distribution for bending loading.

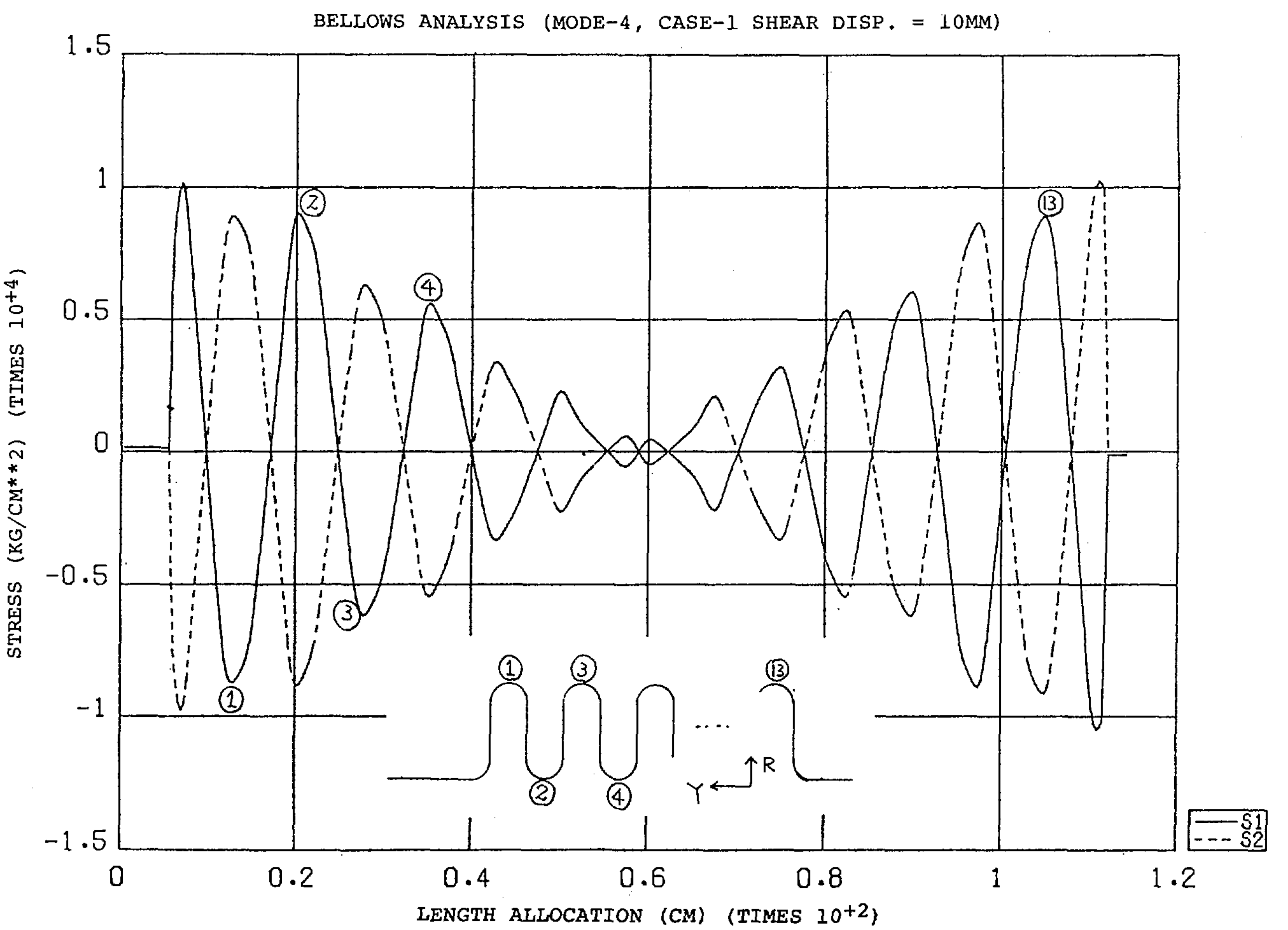

Figure 3-11 Stress distribution for uniform lateral loading.

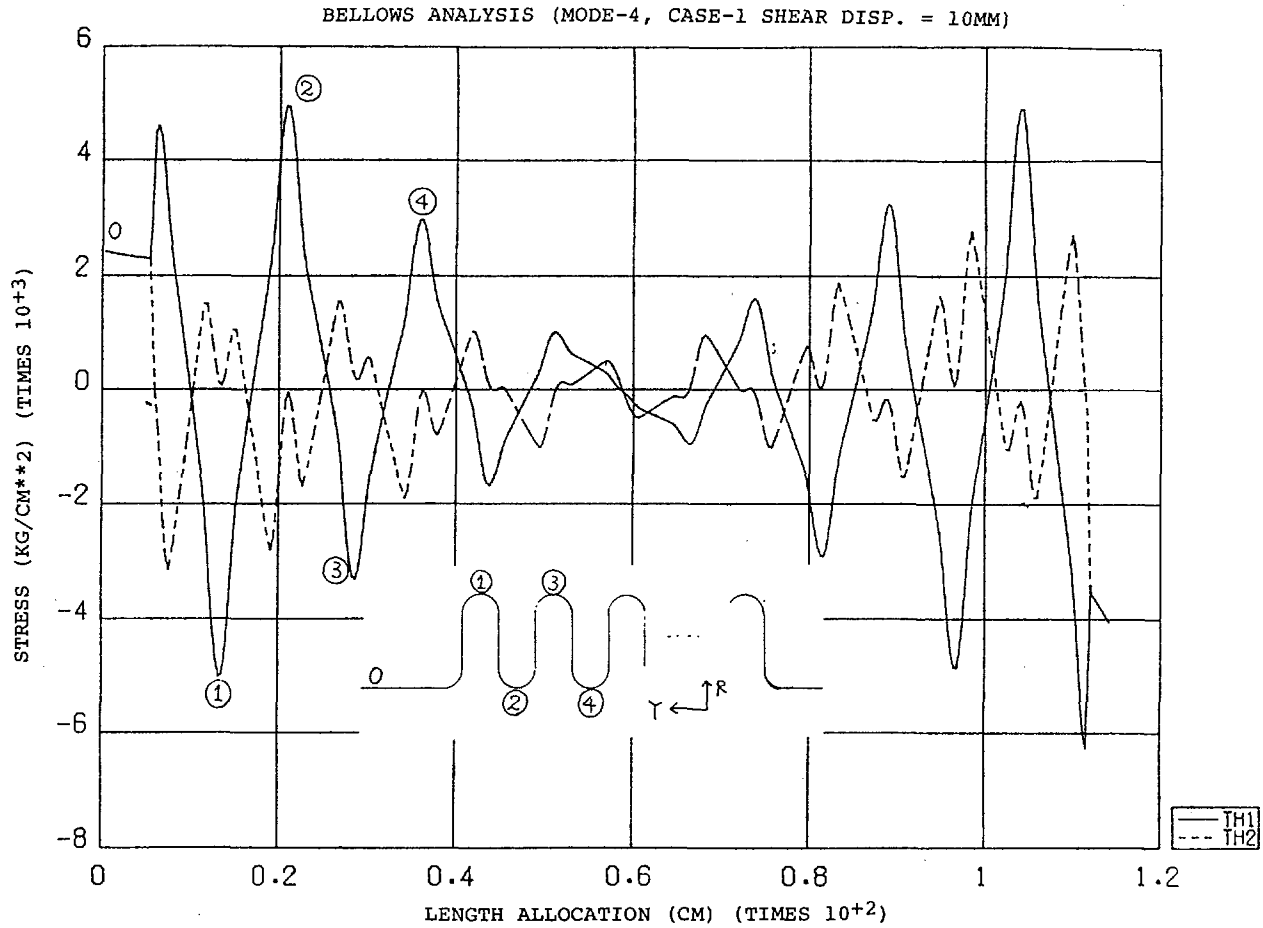

Figure 3-12 Stress distribution for uniform lateral loading.

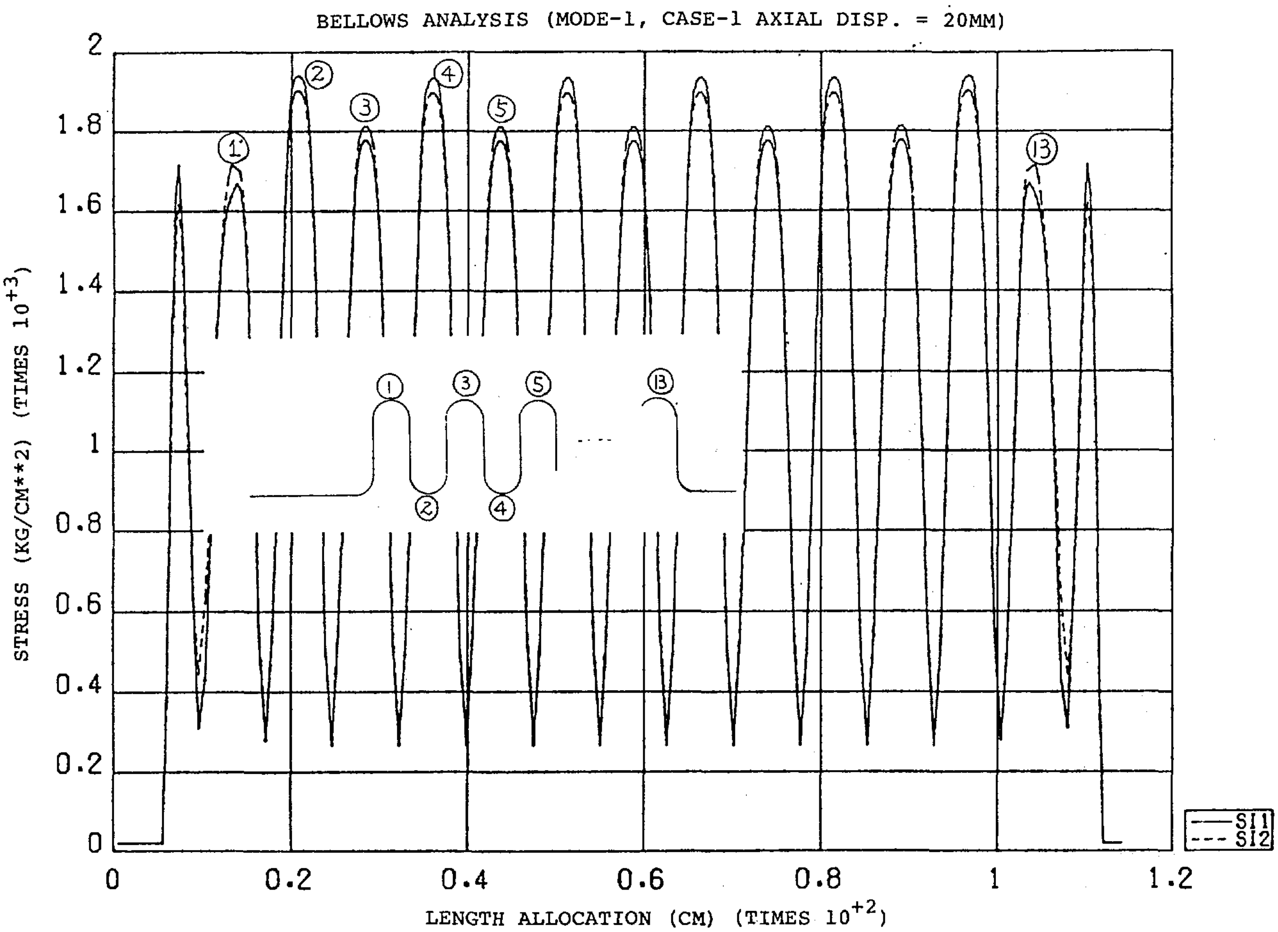

Figure 3-13 Distribution of stress intensity for axial loading.

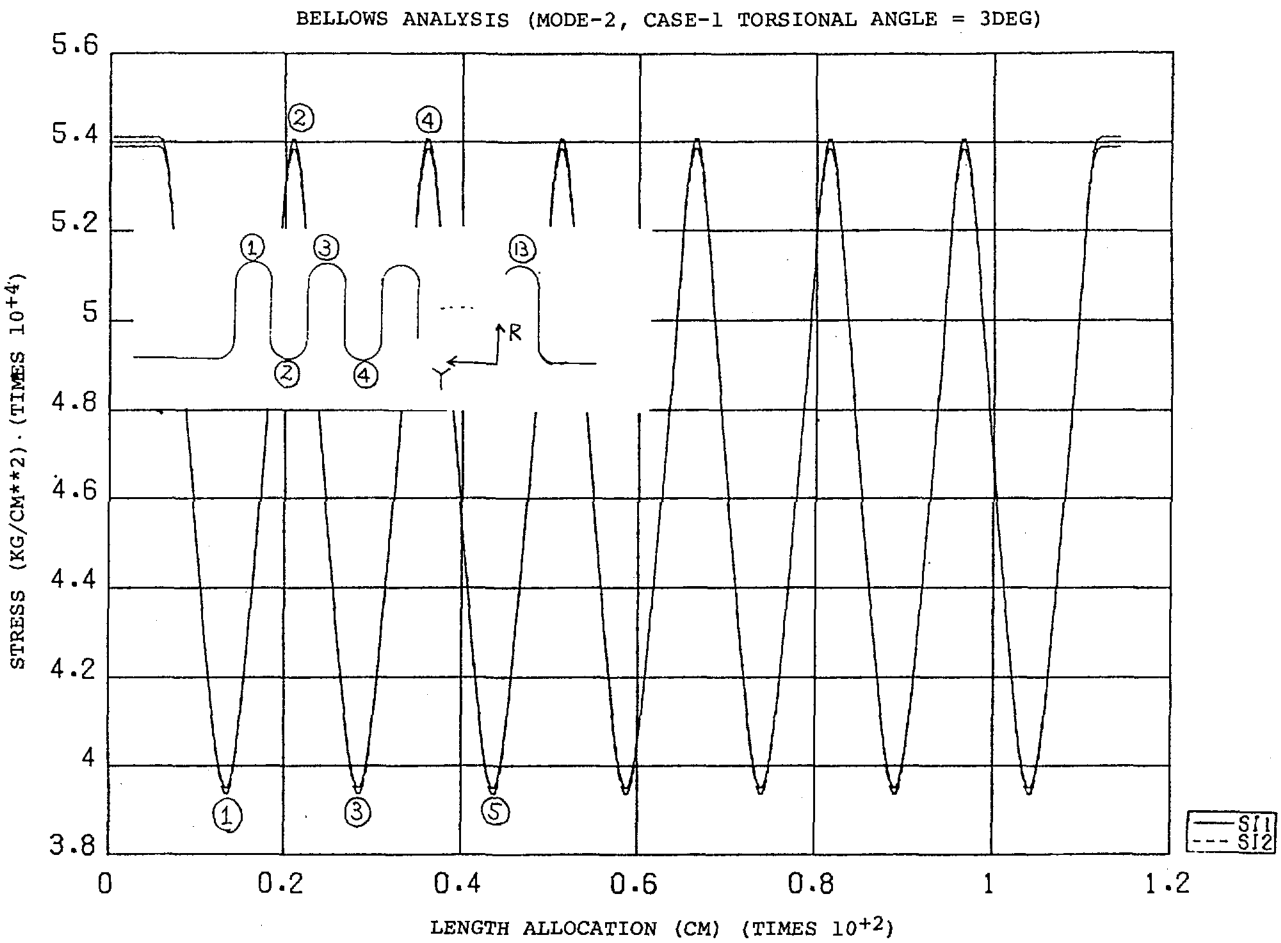

Figure 3-14 Distribution of stress intensity for torsional loading.

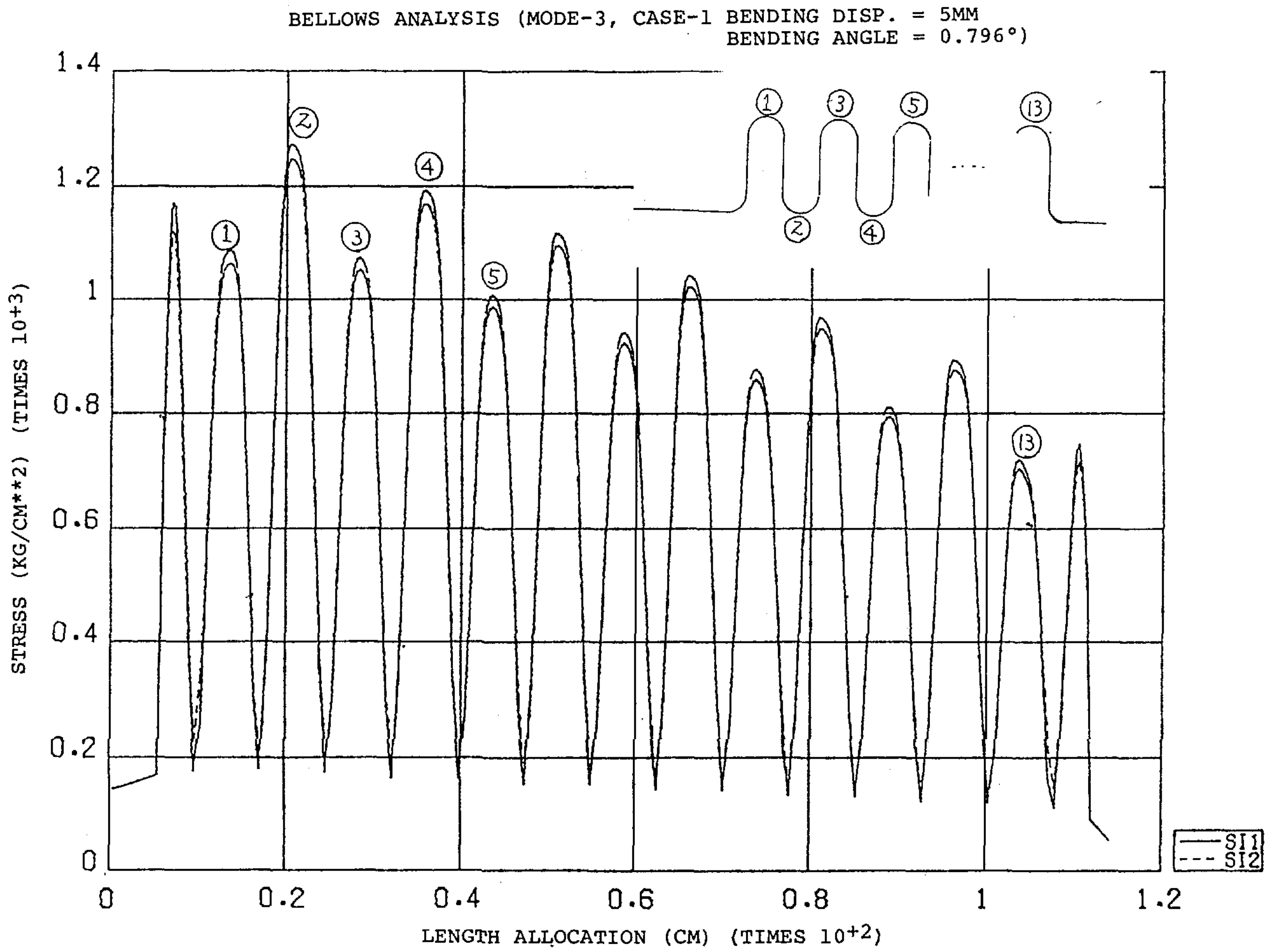

Figure 3-15 Distribution of stress intensity for bending loading.

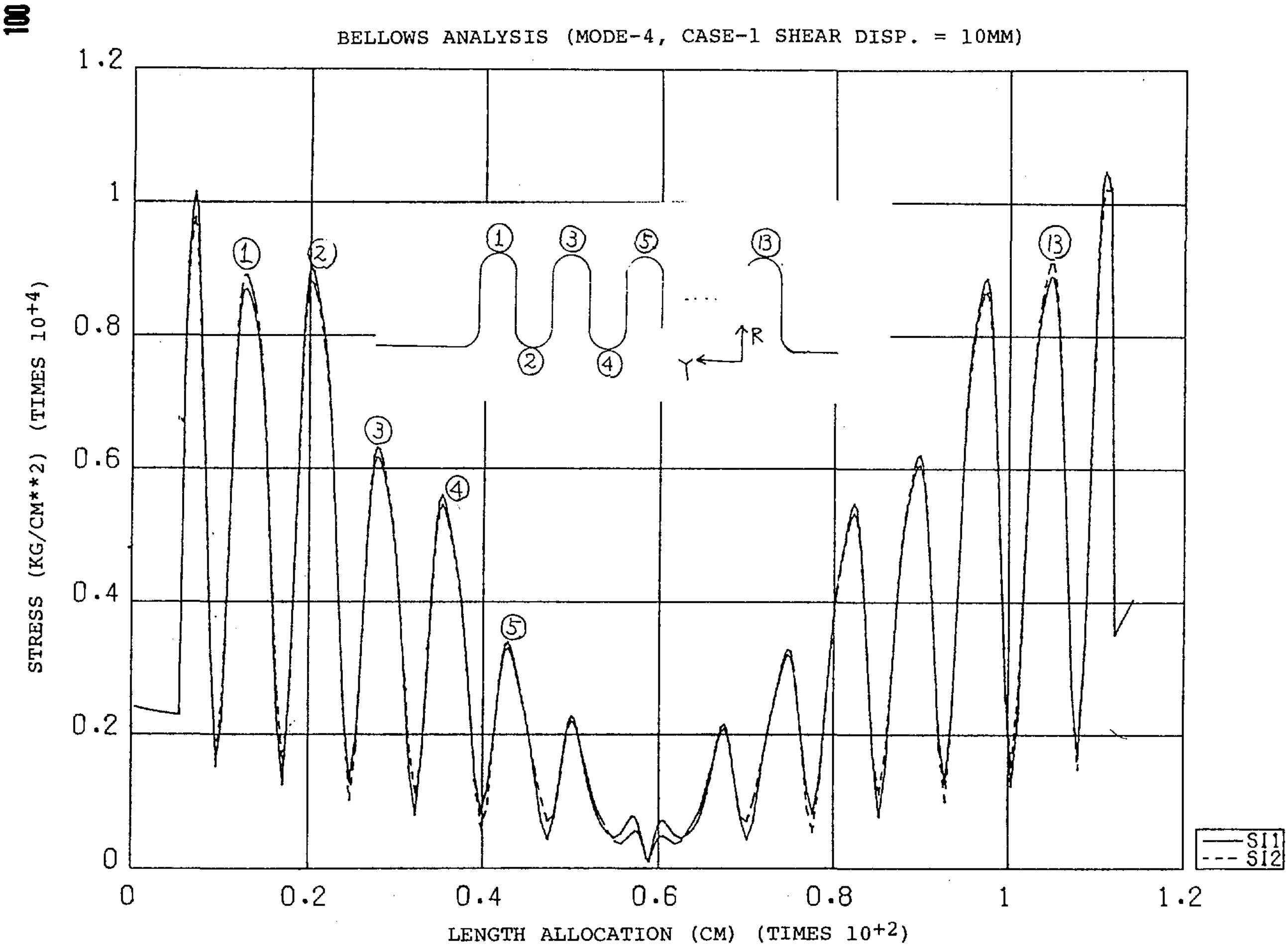

Figure 3-16 Distribution of stress intensity for uniform lateral loading.

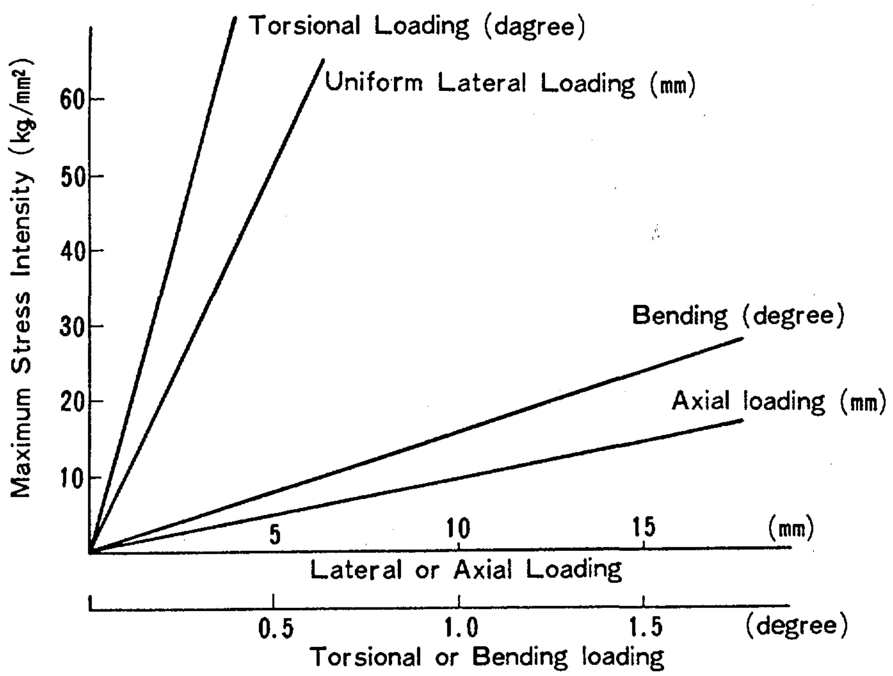

Figure 3-17 Maximum stress intensity VS loadings.